

# Electrical quantum measurement of a two level system at arbitrary voltage and temperature

A. Shnirman<sup>1,2</sup>, D. Mozysky<sup>2</sup>, and I. Martin<sup>2</sup>

<sup>1</sup>Institut für Theoretische Festkörperphysik, Universität Karlsruhe, D-76128 Karlsruhe, Germany

<sup>2</sup>Theoretical Division, Los Alamos National Laboratory, Los Alamos, NM 87545, USA

We calculate the noise spectrum of the output signal of a quantum detector during continuous measurement of a two-level system (qubit). We generalize the previous results obtained for the regime of high voltages (when  $eV$  is much larger than the qubit's energy level splitting) to the case of arbitrary voltages and temperatures. When  $V$  is large the output spectrum is essentially asymmetric in frequency, i.e., the output signal is no longer classical. In the emission (negative frequency) part of the spectrum the peak due to the qubit's coherent oscillations can be 8 times higher than the background pedestal. For  $V < e\Delta$  and  $T = 0$  the coherent peaks do not appear at all.

## I. INTRODUCTION

The problem of quantum measurements has been around since the early days of quantum mechanics. The recent upsurge in the interest to the quantum computing made it necessary to investigate the properties of the real physical systems used as quantum detectors. Thus far the most developed and successful microscopic detectors are the under-damped SQUIDs (or current biased Josephson junctions) which perform switching (threshold, latching) measurements. These systems were investigated for many years. Recently such measurements were used to confirm the coherent dynamics and manipulations of the superconducting qubits<sup>1,2,3,4</sup>. Other measuring devices operate in a smoother mode similar to a (linear) amplifier. Especially interesting are electrometers whose conductance depends on the charge state of a nearby qubit. Two families of electrometers working in this regime have mostly been discussed in the literature. These are the single electron (Cooper pair) transistors (SET)<sup>5,6,7,8,9,10,11,12</sup> and the quantum point contacts (QPC)<sup>13,14,15,16,17,18,19,20,21,22</sup>. Some of these schemes have been implemented experimentally and used for quantum measurements<sup>23,24,25,26,27,28</sup>.

In general one distinguishes between strong and weak quantum measurements. In the strong (von Neumann) measurement the meter discriminates between the states of a qubit on a time scale much shorter than the other time scales of the system, e.g., the inverse level splitting of the qubit. Thus the qubit's internal dynamics is irrelevant and the meter determines the basis in which the measurement takes place (the eigenbasis of the measured observable). Such measurements strongly resemble projection of the qubit's state even though everything can be described by treating the coupled system of the qubit and the meter quantum mechanically. In the opposite, weak measurement limit, the measurement time is relatively long and the state of the qubit may in principle change during the measurement. Yet, there is a special regime in which the measurements resemble projection. This is the so called quantum non-demolition (QND) limit. For example, if the coupling is longitudinal, i.e., if a spin

(qubit) is placed in a magnetic field along the z-axis, and the detector is measuring the  $S_z$  observable of the spin, and there is no extra environment capable of flipping the spin, then  $S_z$  is conserved (non-demolition) and can be measured even if it takes a long time. In all other weak coupling regimes the meter cannot extract precise information about the initial state of the qubit. One can only talk about continuous monitoring of the qubit by the meter in which they influence each other. Studying such continuous monitoring, e.g., in the stationary state, is still useful, as one can extract physical characteristics of the meter and of the qubit and later use them for manipulations, projection-like measurements or quantum feedback control of the qubits<sup>29</sup>.

Continuous monitoring in the regime close to QND was considered in Ref.<sup>30</sup>. The small deviation from the QND limit causes rare spin flips. Thus the current (output signal) in the meter shows the "telegraph noise" behavior. In the noise spectrum of the current this translates into a Lorentzian peak around zero frequency. Recently the QND measurements have been considered in the rotating frame of a spin (qubit)<sup>31</sup>. The regime far from QND was the main focus of Refs.<sup>18,32</sup>. This regime is realized, e.g., in the case of the transverse coupling between the qubit and the meter (magnetic field along the z-axis while  $S_x$  is being measured). The possibility to "observe" the coherent oscillations of a qubit was analyzed. While, due to the unavoidable noise, the oscillations can not be seen directly in the output current, the spectral density of the current noise has a peak at the frequency of the oscillations (Larmor frequency, level splitting of the qubit). The laws of quantum mechanics limit the possible height of the peak. In the case of a 100% efficient (quantum limited) detector the peak can be only 4 times higher than the background noise pedestal<sup>18</sup>. The efficiency of the detector reduces the height of the peak further. Such inefficiency implies<sup>5,6,22</sup> that when the detector is used in the QND regime, the measurement time, i.e., the time needed to discriminate between the states of the qubit is longer than the lowest possible limit for this time, i.e., the dephasing time. This, in turn, means that the meter produces more noise than it is necessary for the measure-

ment, or, in other words, that some information obtained by the meter is not transferred to the output signal.

All the results described above were obtained in the limit when the voltage applied to the measuring device is much higher than the qubit's energy level splitting  $eV$ . In particular, in this regime, the "telegraph noise" peak around  $\omega = 0$  is absent in the case of the purely transverse coupling, while in the intermediate regime (between longitudinal and transverse) the two peaks coexist. The output noise spectrum, in the regime  $eV$  is almost symmetric (classical) at frequencies of order and smaller than  $\omega$ . In this paper we relax the condition  $eV$ . We calculate the non-symmetrized current-current correlator in the case of the purely transverse coupling between the qubit and the meter for arbitrary voltage and temperature. At low voltages,  $eV$ , the output noise is essentially asymmetric, i.e., the output signal is quantum. In other words, we have to differentiate between the absorption ( $\omega > 0$ ) and the emission ( $\omega < 0$ ) spectra of the detector (see, e.g. Ref.<sup>33</sup>). Thus, the detector ceases to be a device able to translate quantum information into the classical one, and the way the output is further measured becomes important. The qubit produces two symmetrically placed peaks in the output noise spectrum. The ratio of the peaks' height to the height of the pedestal can reach 8 for the negative frequency peak. We also obtain a small peak at  $\omega = 0$  (even for purely transverse coupling).

The rest of the paper is organized as follows. In the next section we define the physical system and outline the computational scheme. In Section III, we derive general expressions for average current and fluctuations spectrum, valid for any voltage and temperature. In section IV we provide results for the specific model of a qubit transversely coupled to a quantum point contact. In the appendices we establish connections and clarify distinctions between the technique developed here and the other existing approaches. In Appendix A we analyze the validity of the MacDonald's formula for the current noise in our case. In Appendix B we analyze the applicability of the Bloch-Redfield approximation. In Appendix C we outline the perturbation theory based on spin representation by Majorana fermions.

## II. THE SYSTEM

We study the quantum measurement process in which a quantum point contact (QPC) is used as a measuring device. These devices are known to serve as effective meters of charge (see, e.g., Refs.<sup>23,34,35,36</sup>). In this paper we consider the simplest limit of a tunnel junction when the transmissions of all the transport channels is much smaller than unity and is controlled by the quantum state of a qubit. This model has previously been used by many authors<sup>14,16,20</sup>. The measuring properties of QPCs in a more general case of open channels have been studied, e.g., in Refs.<sup>21,22</sup>.

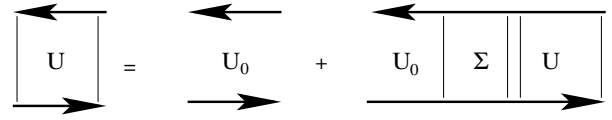


FIG. 1: Dyson equation.

The tunnel junction limit is described by the following Hamiltonian

$$H = \sum_l c_l^\dagger c_l + \sum_r c_r^\dagger c_r + H_{\text{sys}} + \sum_{lr} (c_r^\dagger c_l e^{ik} + \text{h.c.}); \quad (1)$$

where the tunneling amplitude may in principle depend on any operator of the measured system (qubit). In this paper we focus on the case of transverse coupling between the meter and the qubit

$$H_{\text{sys}} = \sum_z (1=2) z \quad (2)$$

$$= T_0 + T_1 x; \quad (3)$$

which is optimal for "observation" of the qubit's coherent oscillations. The transmission amplitudes  $T_0$  and  $T_1$  are assumed to be real positive (as the phase of the transmission amplitude does not matter in our case) and small (tunnel junction limit). Obviously, we only have to consider  $T_1 < T_0$ . We do not, however, assume  $T_1 \ll T_0$ , i.e., we allow for the detectors with large (relative to the average output) response. We have also introduced the counting operator:  $e^{ik} j_n i = j_n + li$ , where  $m$  is the number of electrons that have tunneled through the point contact. Using this trick we could in principle study the full counting statistics of the current<sup>37</sup>.

Following Ref.<sup>38</sup> we integrate out the microscopic degrees of freedom (the electrons) in the left and the right leads and consider the time evolution of the reduced density matrix of the system. This density matrix is a function of the measured system's coordinates as well as of the variable  $m$ , i.e.,  $\hat{\rho} = \hat{\rho}(m_1; m_2)$ . Due to the translational invariance with respect to  $m$  it is convenient to perform the Fourier transform  $\hat{\rho}(k_1; k_2) = \sum_{m_1, m_2} \hat{\rho}(m_1; m_2) e^{ik_1 m_1 + ik_2 m_2}$ . In this representation the operators  $e^{ik}$  in Eq. (1) are diagonal. The master equation for the density matrix with the information about the number of electrons that have tunneled was used in Ref.<sup>14</sup>. Here we do the same in the Fourier space ( $k_1$  and  $k_2$  indexes). We write down the Dyson equation for the propagator of the density matrix (see Fig.1). Taking the time derivative, one arrives<sup>38</sup> at the generalized master equation

$$\frac{d}{dt} \hat{\rho}(t) = L_0 \hat{\rho}(t) = \int_{t_0}^t dt' (t - t') \hat{\rho}(t'); \quad (4)$$

with the zeroth order Liouvillian

$$L_0 = 1 - iH_0^T - iH_0 - 1; \quad (5)$$

Throughout the paper we assume  $\epsilon = 1$ . As we have integrated over the electronic degrees of freedom, the Liouvillian  $L_0$  as well as the Hamiltonian  $H_0$  operate in the direct product of the spin's ( $j = \uparrow, \downarrow$ ) and the counting ( $j = 1, 2$ ) Hilbert spaces. As in the counting space the zeroth Hamiltonian is zero (the number  $m$  changes only due to the tunneling) we have  $H_0 = H_{sys}$  (mathematically rigorously one should write  $H_0 = H_{sys} - 0$ ). We have chosen to present the Liouvillian as a super-operator acting from the left on the density matrix regarded as a vector. This way of writing makes the analysis easier and is especially convenient for numerical simulations. As an example, we rewrite the product  $L_0 \hat{\rho}$  in the matrix form:

$$L_0 \hat{\rho} = \begin{pmatrix} 0 & 0 & 1 & 1 & 0 & 1 & 0 & 1 \\ \frac{i}{2} B & 1 & 0 & 0 & 1 & C & B & \hat{A}_{11} \\ \hat{C} & 1 & 0 & 0 & 1 & A & \hat{C} & \hat{A}_{12} \\ 0 & 1 & 1 & 0 & 1 & A & \hat{C} & \hat{A}_{21} \\ 0 & 1 & 1 & 0 & 1 & A & \hat{C} & \hat{A}_{22} \end{pmatrix} : \quad (6)$$

In the lowest non-vanishing approximation (second order in the tunneling Hamiltonian) for the self-energy we obtain

$$\begin{aligned} \Sigma(t) = & \\ & + (t) \begin{matrix} u_{k_1} \\ d_{k_2} \end{matrix} U_0(t) \begin{matrix} d_{k_2} \\ u_{k_1} \end{matrix} + (t) \begin{matrix} u_{k_1} \\ d_{k_2} \end{matrix} U_0(t) \begin{matrix} d_{k_2} \\ u_{k_1} \end{matrix} \\ & + (t) \begin{matrix} d_{k_2} \\ u_{k_1} \end{matrix} U_0(t) \begin{matrix} u_{k_1} \\ d_{k_2} \end{matrix} + (t) \begin{matrix} d_{k_2} \\ u_{k_1} \end{matrix} U_0(t) \begin{matrix} u_{k_1} \\ d_{k_2} \end{matrix} \\ & + (t) \begin{matrix} u_{k_1} \\ d_{k_2} \end{matrix} U_0(t) \begin{matrix} u_{k_1} \\ d_{k_2} \end{matrix} + (t) \begin{matrix} u_{k_1} \\ d_{k_2} \end{matrix} U_0(t) \begin{matrix} u_{k_1} \\ d_{k_2} \end{matrix} ; \end{aligned} \quad (7)$$

where  $u_{k_1} = e^{ik_1} u$ ,  $d_{k_2} = e^{ik_2} d$ ,  $u = (1, 0)^T$  and  $d = (0, 1)^T$  and  $U_0(t) = e^{iH_0 t}$ . The superscripts  $u$  and  $d$  stand for the "up" and "down" Keldysh contours. We observe that all the matrix elements of the self-energy  $\Sigma(t)$  in Eq. (7) are functions of  $k = k_1 = k_2$  only, i.e., they describe transitions which conserve  $m_1 = m_2$ . In particular they connect the diagonal elements ( $m_1 = m_2$ ) with only the diagonal ones. Even though we could have multiplied the factors  $e^{ik_{1=2}}$  in Eq. (7) and express as function of  $k$ , we keep these factors separately in this particular formula for future convenience. We also introduce the correlators

$$+ (t) = \langle X(t) X^\dagger(0) \rangle ; \quad (8)$$

and

$$(t) = \langle X^\dagger(t) X(0) \rangle ; \quad (9)$$

where  $X = \begin{pmatrix} P \\ \dots \\ C_1 \end{pmatrix}$ . Their Fourier transforms are:

$$+ (!) = (! + V) \frac{1}{2} \coth \frac{! + V}{2T} + \frac{1}{2} ; \quad (10)$$

and

$$(!) = (! - V) \frac{1}{2} \coth \frac{! - V}{2T} + \frac{1}{2} ; \quad (11)$$

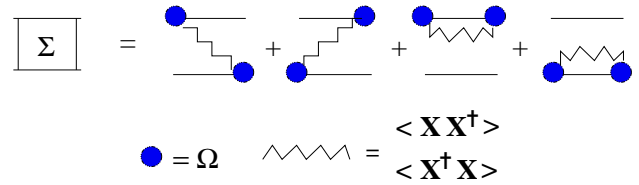


FIG. 2: The first order approximation for the self-energy.

where  $\Sigma = \Sigma_L + \Sigma_R$ . Fig. 2 shows the diagrams that lead to Eq. (7).

Formally, Eq. (4) can be solved by applying the Laplace transformation (that is, it becomes a simple system of linear equations for each value of  $s$ ):

$$\hat{\rho}(k_1; k_2; s) = U(s; k) \hat{\rho}_0 ; \quad (12)$$

where

$$U(s; k) = (s - L_0(k; s))^{-1} ; \quad (13)$$

and  $\hat{\rho}_0$  is the density matrix at  $t = t_0$ .

Further approximations are sometimes used to make them a Markovian. When the dissipative processes are slow in comparison with the unperturbed coherent (Hamiltonian) dynamics, the Bloch-Redfield approximation is appropriate. Within this approximation one substitutes  $\hat{\rho}(t) \approx e^{L_0(t-t_0)} \hat{\rho}_0$  in the RHS of Eq. (4). This leads to  $\Sigma_{BR}$  in Eq. (13), where

$$\Sigma_{BR} = \int_0^t dt \langle X(t) X^\dagger(t_0) \rangle e^{L_0(t-t_0)} ; \quad (14)$$

In our case the validity domain of this approximation extends also to the regime when the dissipative rates are bigger than  $\Gamma$ , i.e., when the qubit is over-damped. Below we will see that, due to the smallness of  $T_0$  and  $T_1$ , the qubit can become over-damped only at high voltages or temperatures, i.e., when  $V \gg T$ . In that case, however, the self-energy  $\Sigma(t-t_0)$  decays on the time scale of order  $1/V$  or  $1/T$  and, thus, is Markovian for slower processes. As we are mostly interested in frequencies not much higher than  $\Gamma$ , we can still use  $\Sigma_{BR}$ . In this paper we will mostly employ the Bloch-Redfield approximation, which gives very simple and transparent results. In Appendix B, however, we will use the non-Markovian expression (13) to confirm that the non-Markovian corrections are small.

As an example of the Bloch-Redfield approximation, let us consider the regime  $V \gg T$  and  $T = 0$ . Then, for  $j = \uparrow, \downarrow$  one has  $+ (!) = (V + !)$ , i.e.,  $+ (t) = (V(t) + i^0(t))$ , while  $(!) = 0$ , i.e.,  $(t) = 0$ . Then using the definition (14) we obtain

$$\begin{aligned} \Sigma_{BR} = & \frac{V}{2} 2e^{ik} \langle u_d u_u \rangle \langle u_u u_d \rangle \\ & + \frac{i}{2} e^{ik} \langle u_d [L_0; d] \rangle \langle e^{ik} d [L_0; u] \rangle \\ & + \frac{i}{2} \langle u_u [L_0; u] \rangle \langle d [L_0; d] \rangle \\ & + i \langle C_1(0) \rangle \langle u_u u_d \rangle ; \end{aligned} \quad (15)$$

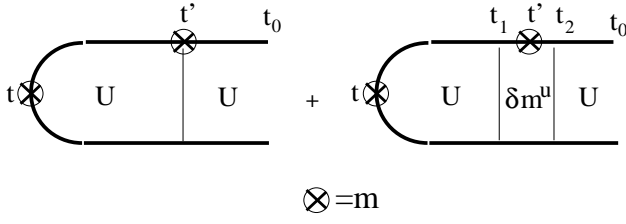


FIG. 3: Diagrammatic representation of the correlator  $\langle m(t)m(t^0) \rangle$ .

where the "value of the delta function at zero",  $\delta_c(0)$ , should be understood as a constant depending on the high energy cut-off  $\Lambda_c$  (diverging with it). Note that  $\delta_c^d = \delta_c^u$ . The last term of Eq. (15) can be rewritten as  $\delta_c(0) [\dots]$ . Thus, this is a renormalization of the spin's Hamiltonian. This renormalization is usually disregarded either because it is small or, as in Caldeira-Leggett's approach, since a counter term has been already added in the initial Hamiltonian. Substituting the self-energy of Eq. (15) into Eq. (4) we arrive at the generalized master equation obtained in Ref.<sup>39</sup> by other technique.

### III. CALCULATION FOR ANY VOLTAGE AND TEMPERATURE

We start by writing down the formally exact expression for the correlator  $\langle m(t)m(t^0) \rangle$  for  $t > t^0$  (see Fig. 3):

$$\begin{aligned} \langle m(t)m(t^0) \rangle &= \text{Tr} [m^u U(t; t^0) m^u U(t^0; t_0) \hat{\rho}_0] \\ &+ \int_{t^0}^t dt_1 \int_{t_0}^{t_1} dt_2 \text{Tr} [m^u U(t; t_1) m^u(t_1; t^0; t_2) U(t_2; t_0) \hat{\rho}_0]; \end{aligned} \quad (16)$$

where  $m^u(t; t^0; t_1) = i\beta \partial_{k_1}$  is the bare vertex  $m^u$  on the upper Keldysh branch while  $m^u(t_2; t^0; t_1)$  is the vertex correction. The importance of the vertex corrections was recently pointed out in Ref.<sup>10</sup>. The  $\text{Tr}[\dots]$  operator is the trace of the density matrix (not of the supermatrices like  $R$ ). The trace over the  $k_{1,2}$  indexes is calculated as  $\frac{dk_1 dk_2}{(2\pi)^2} 2 \delta(k_1 - k_2) \dots$ . For the stationary state properties, which do not depend on the initial density matrix, the trace operator over  $k_{1,2}$  reduces to taking the limit  $k \rightarrow 0$ . This follows from the fact that all the propagators depend on  $k$  only.

For the vertex correction we use the same approximation we have employed for the self-energy (7) (see Fig. 4). One easily obtains  $m^u(t_1; t^0; t_2)$  from Eq. (7) inserting the operator  $m^u$  in all the terms between the operators (from either side of  $U_0$  as  $m^u$  commutes with  $U_0$ ):

$$m^u(t_1; t^0; t_2) = \int_{k_1}^u U_0(t_1 - t_2) m^u \int_{k_2}^d + \dots; \quad (17)$$

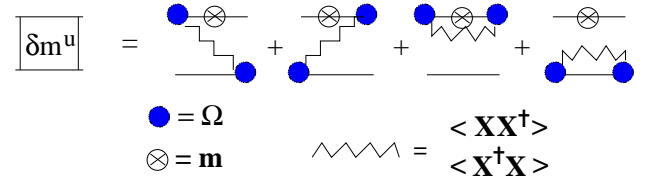


FIG. 4: The first order approximation for the vertex correction.

where  $\dots$  stand for seven more terms obtained in the same way from Eq. (7). We observe that  $m^u(t_1; t^0; t_2) = m^u(t_1 - t_2)$  in this approximation does not explicitly depend on  $t^0$ . We differentiate Eq. (16) over  $t^0$  and use the master equation (4) written in the form  $dU/dt = (L_0 + \dots)U = U(L_0 + \dots)$  to obtain:

$$\begin{aligned} \langle m(t)I(t^0) \rangle &= \text{Tr} [m^u A(t, t^0) U(t^0; t_0) \hat{\rho}_0] \\ &+ \text{Tr} [m^u f(L_0 + \dots) U A(t^0; t_0) \hat{\rho}_0] \\ &+ \text{Tr} [m^u f(L_0 + \dots) U g(t, t^0) f B U(t^0; t_0) \hat{\rho}_0]; \end{aligned} \quad (18)$$

where  $A = m^u m^u$  and  $B = m^u R_t m^u$ . The convolutions are defined as  $fg = \int_{t^0}^t dt_1 g(t - t_1) f(t_1 - t^0)$  and, analogously,  $fg = \int_{t_0}^{t_1} dt_1 \int_{t^0}^{t_1} dt_2 g(t - t_1) f(t_1 - t_2) h(t_2 - t^0)$ . The symbol  $L_0$  in Eq. (18) should be understood as a local in time kernel, i.e.,  $L_0(t - t') = L_0(t - t' - 0)$ . From Eqs. (7) and (17) we obtain

$$\begin{aligned} A(t) &= \int_{k_2}^d U_0(t) \int_{k_1}^u + \int_{k_1}^u U_0(t) \int_{k_2}^d; \end{aligned} \quad (19)$$

and

$$\begin{aligned} B(t) &= \int_{k_1}^u U_0(t) \int_{k_2}^d + \int_{k_1}^u U_0(t) \int_{k_2}^d \\ &+ \int_{k_1}^u U_0(t) \int_{k_1}^u + \int_{k_1}^u U_0(t) \int_{k_1}^u; \end{aligned} \quad (20)$$

Next we note the following property of the superoperators  $L_0$ ,  $\dots$ , and  $A$ :  $\text{Tr}[L_0 \dots] = 0$ ,  $\text{Tr}[\dots] = 0$ , and  $\text{Tr}[A \dots] = 0$ . This allows us to simplify Eq. (18):

$$\begin{aligned} \langle m(t)I(t^0) \rangle &= \text{Tr} [m^u; A]_{(t, t^0)} U(t^0; t_0) \hat{\rho}_0 \\ &+ \text{Tr} [f[m^u; \dots] U A(t^0; t_0) \hat{\rho}_0] \\ &+ \text{Tr} [f[m^u; \dots] U g(t, t^0) f B U(t^0; t_0) \hat{\rho}_0]; \end{aligned} \quad (21)$$

and the commutators are readily calculated:

$$\begin{aligned} [m^u; A]_{(t)} &= \int_{k_2}^d U_0(t) \int_{k_1}^u + \int_{k_2}^d U_0(t) \int_{k_1}^u; \end{aligned} \quad (22)$$

$$\begin{aligned}
[\hat{m}^u; ]_{(t)} = & \\
& + (t) \int_{k_1}^u U_0(t) \int_{k_2}^d (t) \int_{k_1}^u U_0(t) \int_{k_2}^d : \\
& + (t) \int_{k_2}^d U_0(t) \int_{k_1}^u (t) \int_{k_2}^d U_0(t) \int_{k_1}^u :
\end{aligned} \quad (23)$$

We observe that the super-operators  $A, B, [\hat{m}^u; A]$ , and  $[\hat{m}^u; ]$  do not contain the  $\hat{m}$  operators, i.e., there are no differentiations over  $k_{1,2}$  left in Eq. (21). Thus we can safely perform the limit  $k \rightarrow 0$ . We introduce the functions  $\hat{m}^u(t) = \int_{k_1}^u U_0(t) \int_{k_2}^d (t)$  and  $\hat{m}^d(t) = \int_{k_2}^d U_0(t) \int_{k_1}^u (t)$  and obtain for  $k_1 = k_2$

$$\begin{aligned}
A(t) &= \hat{m}^u(t) \int_{k_1}^u U_0(t) \int_{k_2}^d + \hat{m}^d(t) \int_{k_2}^d U_0(t) \int_{k_1}^u ; \\
B(t) &= \hat{m}^u(t) \int_{k_1}^u U_0(t) \int_{k_2}^d - \hat{m}^d(t) \int_{k_2}^d U_0(t) \int_{k_1}^u ; \\
[\hat{m}^u; A]_{(t)} &= \hat{m}^u(t) \int_{k_1}^d U_0(t) \int_{k_2}^u ; \\
[\hat{m}^u; ]_{(t)} &= \hat{m}^u(t) \int_{k_1}^u U_0(t) \int_{k_2}^d + \hat{m}^d(t) \int_{k_2}^d U_0(t) \int_{k_1}^u :
\end{aligned} \quad (24)$$

Finally, for the stationary state we take  $t_0 \rightarrow -\infty$  and obtain (for  $t > t_0$ )

$$\begin{aligned}
hI(t)I(t_0) &= \text{Tr} [\hat{m}^u; A]_{(t-t_0)} \hat{\rho}_{st}^i \\
&+ \text{Tr} f[\hat{m}^u; ]_{(t-t_0)} U A \hat{\rho}_{t_0} \hat{\rho}_{st}^i \\
&+ \text{Tr} f[\hat{m}^u; ]_{(t-t_0)} U \hat{\rho}_{t_0} fB \hat{\rho}_{st}^i ;
\end{aligned} \quad (25)$$

where by definition  $fB \hat{\rho}_{st}^i = \int_0^{R_1} dt_1 B(t_1) = B(s=+0)$  and  $B(s)$  is the Laplace transform of  $B(t)$ . The stationary density matrix is given by

$$\hat{\rho}_{st} = sU(s; k) \hat{\rho}_{st}^i ; \quad (26)$$

Analogously we find the expression for the average current:

$$hI(t) = \text{Tr} f[\hat{m}^u; ]_{(t-t_0)} U \hat{\rho}_{t_0}^i ; \quad (27)$$

which in the stationary regime becomes:

$$hI = \text{Tr} [f[\hat{m}^u; ] \hat{\rho}_{st}^i] ; \quad (28)$$

Equations (24), (25), and (28) constitute the central result of this chapter. They allow us to calculate the current-current correlator and the average current in the first order approximation for the self-energy and the vertex corrections.

#### IV. AVERAGE CURRENT AND NOISE SPECTRUM

To formulate our results in a compact way it is convenient to introduce the two following functions:

$$\begin{aligned}
s(!) &= \frac{(!) + (!)}{2} = \\
&= \frac{(V+!) \coth \frac{V+!}{2T} + (V-!) \coth \frac{V-!}{2T}}{2} ;
\end{aligned} \quad (29)$$

and

$$\begin{aligned}
a(!) &= \frac{(!) - (!)}{2} = \\
&= \frac{(V+!) \coth \frac{V+!}{2T} - (V-!) \coth \frac{V-!}{2T}}{2} ;
\end{aligned} \quad (30)$$

One can easily check that  $! = (s(!) + !)$ , while  $! = (a(!) + V)$ .

For the average current in the stationary regime we obtain the following expression

$$hI = g_0 V + g_1 V \frac{a(V)}{s(V)} ; \quad (31)$$

where we have introduced the conductances  $g_0 = \frac{T_0^2}{T_0}$  and  $g_1 = \frac{T_1^2}{T_1}$ . If  $T = 0$  the result simplifies. For  $V < T$  we obtain  $hI = g_0 V$ , i.e., no contribution of the qubit. For  $V > T$  we have  $hI = g_0 V + g_1 V (1 - \frac{V^2}{T^2})$ . Finally, for  $V \gg T$  we obtain  $hI = g_0 V + g_1 V = (I_{x=+} + I_{x=-})/2$ , where we have introduced the values of the current corresponding to the two  $x$ -projections of the qubit:  $I_{x=\pm} = (T_0 \mp T_1)^2 V = V (g_0 \mp g_1) \frac{1}{2} \frac{1}{g_0 g_1}$ . This result becomes intuitively clear if one notes that the relevant frequency scale of the tunneling process is equal to  $V$  while the fluctuations of spin's observable  $s_x$  have a characteristic frequency  $T$ . In the regime  $\max[V; T] \ll T$  the spin is mostly in the ground state and the tunneling electrons "see" the quantum mechanical average value of  $s_x$ , i.e., zero. Therefore the system behaves as if there was no spin present, i.e., one should substitute in Eq. (3)

$! = T_0$ . In the opposite regime,  $\max[V; T] \gg T$ , the spin is in the mixed state and the electrons sometimes "see" the spin in the state  $|x\rangle$  and sometimes in the state  $|-\rangle$ . Thus the current is the average of  $I_{x=\pm}$ .

To find the output noise spectrum we perform the Laplace transform of Eqs. (25)

$$\begin{aligned}
hI_s^2 &= \text{Tr} [\hat{m}^u; A]_{(s)} \hat{\rho}_{st}^i \\
&+ \text{Tr} [\hat{m}^u; ]_{(s)} U(s) A(s) \hat{\rho}_{st}^i \\
&+ \text{Tr} [\hat{m}^u; ]_{(s)} U(s) B(+0) \hat{\rho}_{st}^i ;
\end{aligned} \quad (32)$$

and, then, find the Fourier transform of the current-current correlator. This last step is done using Mathematica as the expressions are quite extended. The Laplace transforms of the correlators  $\hat{m}^u(t)$  and  $\hat{m}^d(t)$  contain, as usual, the real and the imaginary parts. It is possible to show that the imaginary part of  $\hat{m}^u$  gives rise to the renormalization of the system parameters, e.g., the Lamb shift of the qubit's level splitting, while the imaginary part of  $\hat{m}^d$  is only important at very high frequencies and it ensures the causality of the meter's response functions (see Appendix C). In what follows we neglect the Lamb shift as it is small compared to  $T$ . The full expression splits into three parts  $hI_s^2 = C_1 + C_2 + C_3$ .

The first term of Eq. (32) does not contain the evolution operator  $U(s)$ . It is, thus, expected to give a non-resonant contribution to the current-current correlator,

ie., the pedestal (shot noise):

$$C_1 = g_0 (s(\omega) + 1) + g_1 \frac{s(\omega + \omega_0) + s(\omega - \omega_0) + 2!}{2} \frac{(2 + s(\omega + \omega_0) + s(\omega - \omega_0))}{2s(\omega)} ; \quad (33)$$

For the symmetrized noise power  $S_I^{\text{shot}}(\omega) = C_1(\omega) + C_1(-\omega)$  we then obtain

$$S_I^{\text{shot}}(\omega = 0) = 2g_0s(0) + 2g_1s(\omega_0) \frac{1}{s^2(\omega_0)} ; \quad (34)$$

The two terms in Eq. (34) clearly correspond to the two terms of Eq. (31). This is a usual situation for the shot noise. Yet, the Fano factors for these two contributions are slightly different (at  $T = 0$  both are equal 1).

The last two terms of Eq. (32) contain the evolution operator  $U(s)$  and, thus, are expected to produce resonant contributions. We, first, employ the Bloch-Redfield approximation, ie., we substitute the self-energy  $\Sigma(s)$  in Eq. (13) by  $\Sigma_{\text{BR}}$ . Then we obtain the two remaining contributions  $C_2$  and  $C_3$ . The contribution  $C_2$  is

$$C_2(\omega) = \frac{(\Gamma^2 - \omega^2)}{(\Gamma^2 - \omega^2)^2 + 4\omega^2\Gamma^2} \frac{1}{1 - \frac{a(\omega) + !a(\omega)}{2V s(\omega)}} ; \quad (35)$$

where

$$g_1 s(\omega) = \frac{P \frac{1}{\Gamma_x} - P \frac{1}{\Gamma_{\#x}}}{4V} s(\omega) \quad (36)$$

is the qubit's dephasing rate, while  $\Gamma = \Gamma_x - \Gamma_{\#x} = 4V \frac{P}{g_0 g_1}$  is the sensitivity of the meter.

In the regime  $\Gamma \gg \omega_0$  we obtain two peaks placed around  $\omega = \pm \omega_0$ . This is how the qubit's damped coherent oscillations are reflected in the output noise. Interestingly, this contribution is symmetric, even though the symmetry should not have been expected in general. An asymmetric contribution would correspond to a change in the current-current susceptibility (finite frequency differential conductance) due to the presence of the spin. Such corrections have usually the Fano shape. As shown in Appendix C the lowest order Fano resonances vanish in our model due to the non-universal behavior of the QPC's response functions.

The contribution  $C_2$  (Eq. (35)) is a product of a Lorentzian and a reduction factor in the brackets. The Lorentzian coincides with the one obtained in Ref.<sup>40</sup>. The reduction factor simplifies for  $T = 0$ . Then, if  $V > \omega_0$ , it is given by  $(1 - \omega^2/V^2)$ , while for  $V < \omega_0$  it is equal to 0. In the last case the measuring device can not provide enough energy to excite the qubit and, therefore, the qubit remains in the ground state and does not produce any additional noise. The ratio between the peak's

height and the pedestal's height is different for positive and negative frequencies. In the limit  $g_1 \gg g_0$ ,  $T = 0$ , and  $V < \omega_0$  we obtain  $C_1(\omega) \approx g_0 V (1 - \omega^2/V^2)$  and  $C_2(\omega) \approx 4g_1 V (1 - \omega^2/V^2)$  and, thus,

$$\frac{C_2(\omega = \omega_0)}{C_1(\omega = \omega_0)} = 4 \left(1 - \frac{\omega_0^2}{V^2}\right) ; \quad (37)$$

For  $\omega_0 > V$  the ratio for the negative frequency peak reaches 8. In this limit, however, the peak's height is zero. For symmetrized spectra the maximal possible ratio is 4 (Ref.<sup>32</sup>). We see that the enhancement of the signal-to-noise ratio is due to the fact that the suppression of the qubit's contribution to the noise by factor  $(1 - \omega^2/V^2)$  is smaller than the suppression of the negative frequency background noise by factor  $(1 - \omega^2/V^2)$ . An interesting question is what exactly is observed in the experiments. If the setup for the measurement of the noise would be absolutely passive, like the photon counters in the u-resonance experiments, it could measure only what the system emits, ie. the noise at negative frequencies<sup>41,42</sup>. Moreover, if one is only interested in the excess noise, ie., in the nonequilibrium addition to the noise power due to the finite transport voltage, then even an active detector may be useful. Namely, as shown in Ref.<sup>43</sup>, if the excess noise power is (almost) symmetric, it can be effectively measured by a finite temperature LCR filter. In our case the excess noise consists of the shot noise,  $C_1 - C_1(V = 0)$ , and the coherent peaks  $C_2$ . While the second contribution is symmetric, the first one is only approximately symmetric in the limit  $g_1 \gg g_0$ . Thus, in this limit, the combination  $C_2 + C_1 - C_1(V = 0)$  can be measured. The question of what can be measured in the regime  $g_1 \approx g_0$ , when the excess noise is essentially asymmetric, will be considered elsewhere.

Note also that far from the resonance, for  $|\omega| \gg V$ , the reduction factor in Eq. (35) becomes negative, creating a very small negative contribution to the current-current correlator. This is an artifact of the Bloch-Redfield approximation. The non-Markovian corrections are expected to compensate this negative contribution so that the correlator is positive and vanishes at high negative frequencies.

As the voltage increases so that  $V \approx \omega_0$ , the peaks given by Eq. (35) start to overlap. Then they form a single peak around  $\omega = 0$  which starts getting narrower. Finally, when  $V \gg \omega_0$ , the width of the peak scales as  $\omega \propto V^{-1}$ . This is the strong measurement or Zeno<sup>44</sup> regime. The meter manages to almost localize the qubit in one of the eigenstates of the measured observable ( $\sigma_x$ ). The rare transitions (jumps) give rise to the "telegraph" noise peak around  $\omega = 0$ . The stronger is the measurement ( $\Gamma$ ) the longer is the average time between the jumps (Zeno effect) and, thus, the narrower is the peak. In this regime the output is classical and the reduction factor plays no role (is equal to unity).

Finally, for the last contribution  $C_3$  we obtain

$$C_3(\omega) = \frac{3}{1 + 4\omega^2}$$

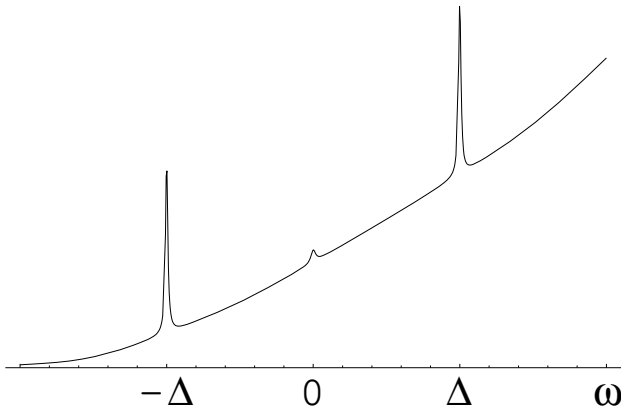


FIG. 5: The output noise for the following parameters:  $V = 1.5$ ,  $T = 0.1$ ,  $g_0 = 0.01$ ,  $g_1 = 0.0064$ .

$$\frac{[a(\omega) + a(-\omega)]}{s^4(\omega)} - 4V s(\omega) - 2 \frac{a(\omega)}{s^2(\omega)} [a(\omega) + a(-\omega)] - s(\omega) [a(\omega) - a(-\omega)] : \quad (38)$$

This contribution corresponds to a small peak around  $\omega = 0$ . For  $T = 0$ ,  $\Delta \ll V$ , and  $V > \omega$  we obtain

$$C_3(\omega) \approx \frac{4}{\omega^2 + 4} \frac{\omega^2}{V^2} - 1 \frac{\omega^2}{V^2} ; \quad (39)$$

while for the same conditions but  $V < \omega$  the contribution  $C_3$  vanishes. To understand the physical meaning of the peak at zero frequency we note, that due to the asymmetry of the correlators and the expectation values of the current corresponding to the two eigenstates of the spin's Hamiltonian  $j_z^+$  and  $j_z^-$  are different (classically they would be equal as in both states  $\langle x_i \rangle = 0$ ). Indeed substituting into Eq. (28) the density matrices  $j_z^+ \rho_z^+$  or  $j_z^- \rho_z^-$  instead of  $\rho_{st}$ , that is forcing the steady state to be one of the eigenstates we obtain for the respective currents  $I = g_0 V + g_1 (V - a(\omega))$ . As the qubit is coherent (under-damped) the back-action noise causes random transitions between the eigenstates of the qubit's Hamiltonian. This translates into the "telegraph" noise of the current. The effect is governed by the ratio  $\omega/V$  and is small in the limit when  $V \gg \omega$ . In the quantum Zeno regime ( $\omega \ll V$ ) the contribution  $C_3$  is always negligible as compared with  $C_1$  and  $C_2$ .

In Fig. 5 we plot an example of the output noise  $\langle I^2 \rangle$ .

## V. CONCLUSIONS

We have calculated the output noise of the point contact used as a quantum detector for arbitrary voltage and temperature. In the regime  $eV \gg T$  and  $T$  the output noise is essentially asymmetric. The qubit's

oscillations produce two peaks at  $\omega = \pm \Delta$ . The peaks have almost equal height and, therefore, the negative frequency peak is much higher relative to its pedestal than the positive frequency one. The peak/pedestal ratio can reach 8. As the negative frequencies correspond to emission, this could be observed by further passive detectors. We have also obtained a "telegraph noise" peak around  $\omega = 0$  for a purely transverse coupling. This peak appears due to the quantum asymmetry of the noise spectra. It means that the detector discriminates not only between the eigenstates of the measured observable ( $x$  in our case) but also between the states of different energy. The results of this paper are obtained for the simplest and somewhat artificial model of a quantum detector. In particular, in this model, the leading contribution of the spin to the output current correlator is of the peak type at all voltages and vanishes at  $V = 0$ . In general this should not be the case, as the coupling to an additional (discrete) degree of freedom usually changes the response functions of the continuum (Fano resonances). In our system, however, certain properties of the response functions of the meter (see Appendix C) prevent the Fano resonances from appearing in the leading order of the perturbation expansion. It would be interesting to perform analogous calculations for more realistic detectors like SET's or QPC's with open channels.

Recently, Bulaevskii, Hruška, and Ortiz<sup>45</sup> studied the problem of a spin in a magnetic field interacting with tunneling electrons with arbitrary spin polarization. They considered the case of low dissipation,  $T \ll eV$ , and the tunneling electrons were coupled to all the projections of the spin operator.

## VI. ACKNOWLEDGMENTS

We thank Yu. Makhlin, G. Schon, D. Averin, M. Buttiker, G. Johansson, A. Rosch, L. Bulaevskii and Y. Levinson for fruitful discussions. A.S. was supported by the EU IST Project SQUBIT, by the DIP (Deutsch-Israelisches Projekt des BMBF), and by the CFN (DFG). D.M. and I.M. were supported by the U.S. DOE.

## APPENDIX A: APPLICABILITY OF THE MACDONALD'S FORMULA

For classical currents it is convenient to use the MacDonald's formula to calculate the noise power of the current. Recently this formula has been applied in Ref.<sup>40</sup> to calculate the output noise of a QPC used as a measuring device (the same system as in this paper). As only the limit  $V \gg T$  was considered, the output signal was classical and the calculation using the MacDonald's formula was well justified. In this Appendix we clarify whether this approach is applicable when the output is quantum.

The MacDonald's formula reads

$$S_I(\omega) = 2! \int_0^{\infty} \frac{dm^2(t)i}{dt} \sin(\omega t) dt; \quad (A1)$$

where  $m^2(t) = \int_0^t I(t') dt'$  is the dispersion of the integral of current  $m = \int_0^t I(t') dt'$ . One starts counting the charge that have tunneled starting from  $t=0$ . One also assumes that at  $t=0$  the spin's density matrix is the stationary one (see Eq. (26)) and that  $m = 0$  at  $t=0$ . Then, since  $\dot{m}(t=0) = 0$ , we obtain

$$S_I(\omega) = \omega^2 [ (s = i\omega + 0) + (s = -i\omega + 0) ] : \quad (A2)$$

To obtain  $\chi(s)$  we apply the propagator  $U(s; k)$  (see Eq. (13)) to the stationary density matrix and, then apply twice the operator  $\hat{m} = i\partial = \partial k$  (as we do it after the propagator, i.e. at the left-most end of the Keldysh contour, we do not distinguish between  $m^u$  and  $m^d$ ). As a result we obtain

$$(s) = \text{Tr} \frac{\partial^2}{\partial k^2} U(s; k) \hat{m} \hat{m}^\dagger : \quad (A3)$$

The derivative over  $k$  in Eq. (A3) can be calculated using Eq. (13):

$$\frac{\partial^2}{\partial k^2} U = U \omega^0 U + 2U \omega^0 U \omega^0 U : \quad (A4)$$

From Eq. (7) it is easy to obtain  $i\omega^0 = [(i\partial = \partial k)]_{k=0} = [m^u; ] = A - B$  (see Eq. (24)) and  $(i^2) \omega^0 = [(i\partial = \partial k)^2]_{k=0} = [m^u; A] + \text{h.c.}$ . After some algebra we conclude that the MacDonald's formula gives for the noise  $S_I$  an expression very similar to the (symmetrized) Eq. (32). However, while in the last line of Eq. (32) there is  $B(+0)$ , the MacDonald's formula puts  $B(s)$  into that place. With this substitution we obtain for the  $C_2$  contribution

$$C_2(\omega) = \frac{(I^2)^2}{(\omega^2)^2 + 4\omega^2} \frac{1}{( + \omega)a( - \omega) + ( - \omega)a( + \omega) + 2!a(\omega)} : \quad (A5)$$

In the classical limit  $\omega = V \rightarrow 0$  the result (A5) coincides with the one obtained in full quantum mechanical calculation (35). However the corrections (even when  $\omega = V$  is small) are not reproduced. Indeed at  $T=0$  and  $\omega < V$  the reduction factor in Eq. (35) is  $(1 - \omega^2/V^2)$  while Eq. (A5) gives  $(1 - \omega^2/2V^2)$ .

#### APPENDIX B: BEYOND THE BLOCH-REDFIELD APPROXIMATION

We have also calculated the output noise without using the Bloch-Redfield approximation, i.e., substituting the

non-Markovian self energy  $\chi(s)$  into Eq. (13). In the regime  $\omega \ll V$  we found the following correction around  $C_2$ :

$$C_2(\omega) \rightarrow \frac{4g_0g_1V(\omega^2 - V^2)}{(\omega^2 - V^2)^2 + 8\omega^2} + \frac{2(g_0 - g_1)V + g_1a(2\omega)(s(\omega))}{s(\omega)} : \quad (B1)$$

This feature has a "Fano" shape and it makes the main peaks (Eq. (35)) a bit asymmetric. As far as the coupling constants (conductances) are concerned, the correction (B1) seems to be of the same order as the terms  $C_2$  and  $C_3$ . Thus, the question arises, what does the Bloch-Redfield approximation exactly mean. Analyzing this question deeper we note, that within this approximation the self-energy  $\chi$  and, consequently, the evolution operator  $U$  factorize into two parts: the part describing the diagonal (in the eigen-basis of the qubit's Hamiltonian) elements of the density matrix (two modes with eigenfrequencies around  $\omega = 0$ ) and the part describing the off-diagonal elements (two modes with eigenfrequencies around  $\omega = \pm V$ ). The first part is responsible for the contribution  $C_3$ , while the second part is responsible for  $C_2$ . The non-Markovian corrections to couple these two pairs of modes. These corrections are, however, proportional to the deviations from the eigenfrequencies, e.g., to  $(\omega - V)$ . Thus, they vanish exactly at the eigenfrequencies. More rigorously, since the width of the resonances is proportional to  $g_1$ , the non-Markovian corrections carry an additional factor of  $g_0$  or  $g_1$  within the resonances. There, the Bloch-Redfield approximation is well justified and the corrections are of the higher order in  $g_0; g_1$ . Outside the resonances the Bloch-Redfield approximation may be not justified. There, however, the main contribution is the shot noise term  $C_1$  which does not depend on  $U(s)$  and is not sensitive to the Bloch-Redfield approximation. In Appendix C we will show, that, indeed, the Fano shaped contribution (B1) is of the higher order than those, that could, in principle, have appeared together with the main peaks (35).

#### APPENDIX C: STANDARD KELDYSH CALCULATION WITH MAJORANA FERMIONS

It is possible to obtain Eqs. (33) and (35) using the standard Keldysh diagrammatic technique<sup>46</sup>. For the two-level (spin-1/2) system it is convenient to employ the mixed Dirac-Majorana-fermion representation (see e.g. Ref<sup>47</sup>):

$$\begin{aligned} \psi &= z f \\ \psi^\dagger &= f^\dagger z \\ z &= 1 - 2f^\dagger f; \end{aligned} \quad (C1)$$

where  $f$  is the Dirac fermion while  $z$  is the Majorana fermion ( $z = (g + g^\dagger)$ ), so that  $f z; z g = 2 (g$  being



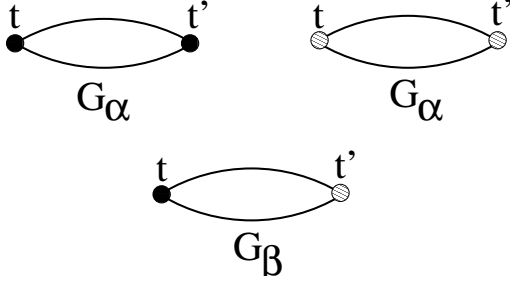


FIG. 6: The graphical representation of the Green's functions  $G_\alpha$  (Eq. (C3)) and  $G_\beta$  (Eq. (C4)). The loops are here to remind that each of these Green's functions is actually a combination of two electronic ones. In the approximations we use the electronic lines appear only in such combinations.

another Dirac fermion)).

Our purpose is to calculate the correlator  $\langle I(t)I(t^0) \rangle$  which can be presented as one of the components of the current-current Green's function  $G_I(t; t^0) = \langle I(t)I(t^0) \rangle$ . Namely

$$\langle I(t)I(t^0) \rangle = i[G_I^{-1}]_{11} = iG_I^{-1} : \quad (C2)$$

In what follows we use the (Keldysh) notations explained in Ref.<sup>48</sup>. The current operator is given by  $I = i(X - X^\dagger)$ , while the tunneling Hamiltonian (the vertex of the perturbation theory) is  $H_T = (X + X^\dagger)$ . It is, thus, convenient to introduce the two following Green's functions:

$$G = \langle I(t)I(t^0) \rangle = \langle i(X - X^\dagger)(t) i(X - X^\dagger)(t^0) \rangle = \langle i(X - X^\dagger)(t) i(X + X^\dagger)(t^0) \rangle ; \quad (C3)$$

and

$$G = \langle i(X - X^\dagger)(t) i(X + X^\dagger)(t^0) \rangle ; \quad (C4)$$

where the subscripts  $>$  and  $<$  point to an obvious relation to the functions  $G^>$  and  $G^<$  introduced above. Indeed  $G^> = \langle I(t)I(t^0) \rangle$  and  $G^< = \langle I(t^0)I(t) \rangle$ , while  $G^> = \langle I(t)I(t^0) \rangle$  and  $G^< = \langle I(t^0)I(t) \rangle$ . The two lines of Eq. (C3) might in principle be different, for example, in the superconducting case. In our case, however they are equal. For these two Green's functions we use the graphical representation shown in Fig. 6.

Finally we introduce the fermionic Green's functions. For the Majorana fermions we define  $G = \langle I(t)I(t^0) \rangle = \langle i\tau_z(t) i\tau_z(t^0) \rangle$ . It is easy to obtain the bare Green's functions  $G^>,0 = \langle I(t)I(t^0) \rangle$  and  $G^<,0 = \langle I(t^0)I(t) \rangle$ . For the fermions it is convenient to use the Bogolubov-Nambu representation, i.e.,  $(f; f^\dagger)^T$  and  $(f^\dagger; f)$  and, then,  $G = \langle I(t)I(t^0) \rangle = \langle i\tau_z(t) i\tau_z(t^0) \rangle$ .

The bosonic functions  $G_\alpha$  and  $G_\beta$  describe the reservoirs and, therefore, are well approximated by their unperturbed values. Making this approximation we neglect

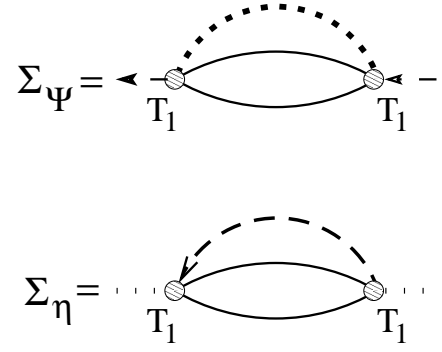


FIG. 7: The lowest order non-vanishing diagrams for the self-energies  $\Sigma_\Psi$  and  $\Sigma_\eta$ . The solid lines are electronic ones, the dashed line is the Green's function of the Dirac (f) fermion and the dotted line is the Majorana fermion's one.

a possibility of the spin-induced correlations in the reservoirs (leads), i.e., the Kondo effect. This is justified if  $\max(T; V) > T_K$ .

The fermionic Green's function  $G$  and  $G$  describe the spin, which can be driven far out of equilibrium. Thus, we find these functions from the (kinetic (Dyson) equations.

$$G^{-1} = G_{;0}^{-1} ; \quad (C5)$$

$$G^{-1} = G_{;0}^{-1} ; \quad (C6)$$

where  $\Sigma_\Psi$  and  $\Sigma_\eta$  are the fermion's and fermion's self-energies respectively. All the quantities in Eq. (C5) are matrices  $4 \times 4$  (in the Nambu and Keldysh spaces). The operator  $G_{;0}^{-1}$  is given by

$$G_{;0}^{-1} = \begin{pmatrix} 0 & 0 & 0 & 1 \\ 0 & 0 & 0 & 0 \\ 0 & 0 & 0 & 0 \\ 0 & 0 & 0 & 0 \end{pmatrix} + \begin{pmatrix} B & C \\ 0 & A \end{pmatrix} ; \quad (C7)$$

while for  $G_{;0}^{-1}$  we obtain

$$G_{;0}^{-1} = \begin{pmatrix} 0 & 0 \\ 0 & 0 \end{pmatrix} ; \quad (C8)$$

In Eqs. (C7) and (C8) we have neglected the infinitesimal terms responsible for, e.g., causality of the Green's functions. These are no longer needed when the finite self-energies are taken into account.

For the self-energies we take the lowest non-vanishing order approximation shown in Fig. 7. As usually, in the Keldysh space the self-energies are presented as

$$\Sigma = \begin{pmatrix} R & K \\ 0 & A \end{pmatrix} ; \quad \Sigma = \begin{pmatrix} R & K \\ 0 & A \end{pmatrix} ; \quad (C9)$$

From Fig. 7 it is easy to conclude that  $\Sigma^> = i\tau_1^2 \hat{G}^> G^>$  and  $\Sigma^< = i\tau_1^2 \hat{G}^< G^<$ , where the Nambu matrix

is defined  $\hat{G} = \begin{pmatrix} 1 & 1 \\ 1 & 1 \end{pmatrix}$ . Analogously we obtain  $\hat{G}^> = iT_1^2 G^> \begin{pmatrix} 1 & 1 \\ 1 & 1 \end{pmatrix} G^> \begin{pmatrix} 1 \\ 1 \end{pmatrix}$  and  $\hat{G}^< = iT_1^2 G^< \begin{pmatrix} 1 & 1 \\ 1 & 1 \end{pmatrix} G^< \begin{pmatrix} 1 \\ 1 \end{pmatrix}$ . To calculate the self-energies in the lowest order we can use the unperturbed retarded and advanced fermionic Green's functions. This is not so for the Keldysh component, which contains the information about the distribution function:  $G^K = (!) = h = (!) G^R = (!) G^A = (!)$ . As was pointed out in Ref.<sup>49</sup> the distribution functions  $h = (!)$  are determined by the reservoirs even in the zeroth order. Thus they should be found self-consistently. After some algebra we find

$$G^R = T_1^2 \hat{G} G^K + h(0) (G^R - G^A) \quad (C10)$$

and

$$G^K = T_1^2 \hat{G} (G^R - G^A) + h(0) G^K : \quad (C11)$$

In what follows we will only need the Green's function  $G^>$ . Therefore, instead of proceeding with the self-consistent determination of the functions  $h =$ , we note that  $h(0) = 0$  just by symmetry (the self-consistent calculation gives the same). Thus we obtain

$$\text{Im } G^R (!) = \hat{G} ! ; \quad (C12)$$

where  $! = g_s(!)$  (see Eq. (36) where we have introduced  $! =$ ). Analogously,  $\text{Im } G^A (!) = \hat{G} (!)$ . The real parts of the retarded and advanced self-energies give the non-equilibrium generalization of the Lamb shift. Here we neglect it. For the Keldysh component we have

$$G^K (!) = 2ig \hat{G} ! : \quad (C13)$$

Substituting the selfenergy into the Dyson equation (C5) we obtain

$$\begin{pmatrix} G^> \\ G^< \end{pmatrix} = \begin{pmatrix} G^> \\ G^< \end{pmatrix} \begin{pmatrix} 1 & 1 \\ 1 & 1 \end{pmatrix} + \begin{pmatrix} 2ig! & 2ig_1! \\ 2ig_1! & 2ig! \end{pmatrix} \begin{pmatrix} 1 \\ 1 \end{pmatrix} ; \quad (C14)$$

which is easy to invert. As a result we obtain

$$G^{R=A} = \frac{\begin{pmatrix} ! + & i! & i! \\ i! & ! & i! \end{pmatrix}}{(!^2 - 2)^2 + 4!^2} ; \quad (C15)$$

$$G^K = \frac{2ig_1! \begin{pmatrix} (! + )^2 & !^2 \\ !^2 & (! )^2 \end{pmatrix}}{(!^2 - 2)^2 + 4!^2} : \quad (C16)$$

Now we are ready to calculate the current-current correlator (C2). The lowest order diagrams contributing to this correlator are shown in Fig. 8. They give

$$G_I^> (t - t^0) = T_0^2 G^> (t - t^0) + iT_1^2 \hat{G}^> (t - t^0) G^> (t - t^0) ; \quad (C17)$$

where

$$\begin{aligned} & i\text{Tr}_K [x(t) x(t^0)] \\ & = i\text{Tr}_K [z f + f^y_z](t) (z f + f^y_z)(t^0) i : \end{aligned} \quad (C18)$$

One obtains Eq. (C17) summing all possible orientations of the lines in Fig. 8.

In the Majorana representation the Green's function is a "two-particle" Green's function (a bubble). To calculate it properly one has to take into account, e.g., the vertex corrections, which seems to be complicated. Instead we use here an identity, recently proven in Refs.<sup>50,51</sup>, which reduces to a single-fermion Green's function.

$$h_x(t) x(t^0) i = h[f(t) + f^y(t)][f(t^0) + f^y(t^0)] i : \quad (C19)$$

From Eq. (C19) it is easy to obtain the following relations

$$\hat{G}^> = \begin{pmatrix} 1 & 1 \\ 1 & 1 \end{pmatrix} G^> \begin{pmatrix} 1 \\ 1 \end{pmatrix} ; \quad (C20)$$

and

$$\hat{G}^< = \begin{pmatrix} 1 & 1 \\ 1 & 1 \end{pmatrix} G^< \begin{pmatrix} 1 \\ 1 \end{pmatrix} : \quad (C21)$$

Performing usual Keldysh manipulations we obtain

$$G^R = \frac{8ig!^2}{(!^2 - 2)^2 + 4!^2} ; \quad (C22)$$

$$G^K = \frac{8i!^2}{(!^2 - 2)^2 + 4!^2} ; \quad (C23)$$

and, finally,

$$\hat{G}^> = \frac{1}{2} (G^K + G^R) = \frac{4ig (s(!) + !)^2}{(!^2 - 2)^2 + 4!^2} : \quad (C24)$$

We then obtain Eq. (33) from Eqs. (C17) and (C24) in the regime  $! =$ . In this case we can approximate  $\hat{G}^>$  by a sum of two delta functions and perform the convolution in the second term of Eq. (C17).

The diagrams giving the peaks at  $! =$  are shown in Fig. 9. They are chosen out of many other second-order diagrams, since only in these diagrams the spin's line (the combined loop of the f and Majorana fermions), which gives the Green's function  $G^>$ , carries the external frequency  $!$ . In all other diagrams the spin's lines participate in loops and are, thus, being integrated over the frequency. Then the resonant structure is washed out and one merely gets a second order correction to the shot noise (pedestal). Although in Fig. 9 we draw the loops

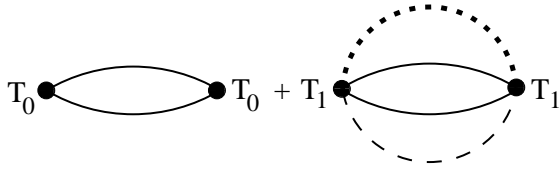


FIG. 8: The diagrams leading to Eq. (33). The f-line should be found from the Dyson (kinetic) equation as in Ref.<sup>49</sup>.

(bubbles) of f and  $\zeta$  lines, we do not actually calculate those but use instead Eqs. (C 22) and (C 23).

It is quite easy to calculate the first diagram (Fig. 9a). It is given by  $T_0^2 T_1^2 G^A(\omega) [G^R(\omega)]$ . In the other three diagrams the internal vertices, over which the integration is performed, are not further connected. Let us, for example consider the diagram b). Acting, first, in the (11;12;21;22) Keldysh coordinates (see Ref.<sup>48</sup>) we see that the left electronic loop of this diagram, after integration over the time of the "free" vertex, gives a "Keldysh vector"  $\hat{D}_j$ , where j is the Keldysh index of the left external vertex. Thus the whole diagram b) can be presented as  $T_0^2 T_1^2 \hat{D}_j \hat{D}_{jk}$  (no summation over j), where  $\hat{D}$  denotes the rest of the expression which can be treated as a usual Keldysh matrix ( $\hat{D}$  in this case is given by  $[G^A]$  in the (R;A;K) coordinates). For  $\hat{D}_j$  we obtain  $\hat{D}_j = [G^R(\omega)]_{1j} [G^A(\omega)]_{j2} = G^A(\omega)$ . Thus  $\hat{D}_j$  is actually a (Keldysh) scalar and the diagram b) can be, finally, calculated as  $T_0^2 T_1^2 [G^A(\omega)] [G^R(\omega)]$ . Collecting the rest of the diagrams we obtain the following contribution to the current-current Green's function

$$G_I = T_0^2 T_1^2 [G^A(\omega) \hat{D}(\omega) [G^R(\omega) \hat{D}(\omega) G^A(\omega)]] : \quad (C 25)$$

We calculate the Keldysh components of the Green's function  $G^A$  for  $\omega \ll D$ , where  $D = \frac{1}{L=R}$  is the electronic bandwidth (the Fermi energy). As a result we obtain:  $G^R(\omega) = V [1 + i0 (\omega = D)]$ ,  $G^A(\omega) = V [1 - i0 (\omega = D)]$ , and  $G^K(\omega) = 2a(\omega)$ . The factors  $1 \pm i0 (\omega = D)$  are responsible for making the functions  $G^R(t)$  and  $G^A(t)$  causal. As we are interested in the low frequencies ( $\omega \ll D$ ) we approximate those factors by 1. Then we obtain

$$G_I = 4g_0 g_1 \begin{pmatrix} V a(\omega) & R & K & 0 & a(\omega) \\ 0 & 0 & A & 0 & V \end{pmatrix} ; \quad (C 26)$$

and, finally,  $G_I^{R=A} = 0$  and

$$G_I^K = 2 G_I^> = 4g_0 g_1 V^2 \begin{pmatrix} a(\omega) \\ V \end{pmatrix} (R \quad A) : \quad (C 27)$$

The first term in Eq. (C 27) is the standard contribution obtained in the high voltage limit, e.g., in Refs.<sup>18,32</sup>. It can also be obtained by treating the QPC as a linear amplifier, i.e., assuming the relation  $I(t) = I_0(t) + \frac{I}{2} x(t)$ <sup>52</sup>.

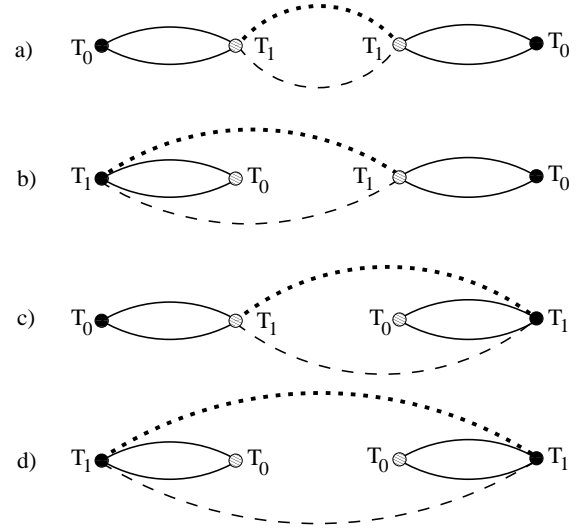


FIG. 9: The diagrams leading to Eq. (35). The solid lines are electronic ones, the dashed line is the Green's function of the Dirac fermion and the dotted line in the Majana fermion's one.

Then, the first term in Eq. (C 27) is the noise of the spin being amplified by the QPC. The interpretation of the second term in Eq. (C 27) is less trivial. Now these are the internal correlations of the QPC being amplified by the combined system of the spin and the QPC. This contribution is negligible when  $\omega \ll V$  but is of the same order as the first one for  $\omega \sim V$ . Using Eqs. (C 22) and (C 23) we, finally, obtain the following contribution to the current-current correlator

$$i G_I^> = \frac{(I^2 \omega^2)^2}{(I^2 \omega^2)^2 + 4 \omega^2 I^2} \frac{1}{V S(\omega)} : \quad (C 28)$$

The contribution (C 28) coincides with  $C_2(\omega)$  (Eq. (35)) in the limit  $\omega \ll V$ .

Note that the response functions  $G^R(\omega)$  and  $G^A(\omega)$  vanish at  $V = 0$ . This non-universal property makes the spin's contribution to the equilibrium output current correlator to vanish. At any voltage and temperature, the contribution (C 28) is of the "peak" type, and not of the Fano type. The Fano shaped resonances could have originated from the combination  $R + A = 2\text{Re } R$ . Indeed, for  $\omega \ll V$  and  $j! j$  we obtain from Eq. (C 22)

$$R + A = \frac{4 \omega^2}{S(\omega)} \frac{\omega^2}{(I^2 \omega^2)^2 + 4 \omega^2 I^2} : \quad (C 29)$$

This combination does not appear in Eq. (C 28) due to another non-universal property of the response functions  $G^R(\omega)$  and  $G^A(\omega)$  which are purely real up to the frequencies of order  $D$ . Had this not been the case, the Fano type contribution would be similar to that of Eq. (B 1) but of a lower order in  $g_0; g_1$  ( $\propto g_0 g_1$ ).

- <sup>1</sup> D. Vion, A. Aassime, A. Cottet, P. Joyez, H. Pothier, C. Urbina, D. Esteve, and M. H. Devoret, *Science* 296, 886 (2002).
- <sup>2</sup> Y. Yu, S. Han, X. Chu, S. Chu, and Z. Wang, *Science* 296, 889 (2002).
- <sup>3</sup> J. M. Martinis, S. Nam, J. Aumentado, and C. Urbina, *Phys. Rev. Lett.* 89, 117901 (2002).
- <sup>4</sup> I. Chiorescu, Y. Nakamura, C. J. P. M. Harmans, and J. E. Mooij, *Science* (2002).
- <sup>5</sup> A. Shnirman and G. Schon, *Phys. Rev. B* 57, 15400 (1998).
- <sup>6</sup> M. H. Devoret and R. J. Schoelkopf, *Nature* 406, 1039 (2000).
- <sup>7</sup> D. Averin, *cond-mat/0010052* (2000).
- <sup>8</sup> Yu. Makhlin, G. Schon, and A. Shnirman, *Rev. Mod. Phys.* 73, 357 (2001).
- <sup>9</sup> A. M. Aassen van den Brink, *Europhys. Lett.* 58, 562 (2002).
- <sup>10</sup> G. Johansson, A. Kock, and G. Wendin, *Phys. Rev. Lett.* 88, 046802 (2002).
- <sup>11</sup> A. Clerk, A. N. S. M. Girvin, and A. Stone, *Phys. Rev. Lett.* 89, 176804 (2002).
- <sup>12</sup> G. Johansson, *cond-mat/0210539* (2002).
- <sup>13</sup> I. L. Aler, N. S. Wingreen, and Y. M. R. Phys. Rev. Lett. 79, 3740 (1997).
- <sup>14</sup> S. A. Gurvitz, *Phys. Rev. B* 56, 15215 (1997).
- <sup>15</sup> Y. Levinson, *Europhys. Lett* 39, 299 (1997).
- <sup>16</sup> A. N. Korotkov, *Phys. Rev. B* 60, 5737 (1999).
- <sup>17</sup> M. Buttiker and A. Martin, *Phys. Rev. B* 89, 2737 (2000).
- <sup>18</sup> A. N. Korotkov and D. V. Averin, *Phys. Rev. B* 64, 165310 (2001).
- <sup>19</sup> H. S. Goan, G. J. M. Ilum, H. M. Wiseman, and H. B. Sun, *Phys. Rev. B* 63, 125326 (2001).
- <sup>20</sup> H. S. Goan and G. J. M. Ilum, *Phys. Rev. B* 64, 235307 (2001).
- <sup>21</sup> S. Pilgram and M. Buttiker, *Phys. Rev. Lett.* 89, 200401 (2002).
- <sup>22</sup> A. Clerk, S. Girvin, and A. Stone, *Phys. Rev. B* 67, 165324 (2003).
- <sup>23</sup> E. Buks, R. Schuster, M. Heiblum, D. Mahalu, and V. Umansky, *Nature* 391, 871 (1998).
- <sup>24</sup> R. J. Schoelkopf, P. Wahlgren, A. A. Kozhevnikov, P. Delsing, and D. E. Prober, *Science* 280, 1238 (1998).
- <sup>25</sup> Y. Nakamura, Yu. A. Pashkin, and J. S. Tsai, *Nature* 398, 786 (1999).
- <sup>26</sup> D. Sprinzak, E. Buks, M. Heiblum, and H. Shtrikman, *Phys. Rev. Lett.* 84, 5820 (2000).
- <sup>27</sup> A. Aassime, G. Johansson, G. Wendin, R. J. Schoelkopf, and P. Delsing, *Phys. Rev. Lett.* 86, 3376 (2001).
- <sup>28</sup> D. Gunnarsson, T. Duty, K. Bladh, R. Schoelkopf, and P. Delsing, *Proceedings of LT 23, Hiroshima* (2002).
- <sup>29</sup> R. Ruskov and A. Korotkov, *Phys. Rev. B* 66, 041401(R) (2002).
- <sup>30</sup> Yu. Makhlin, G. Schon, and A. Shnirman, *Phys. Rev. Lett.* 85, 4578 (2000).
- <sup>31</sup> D. V. Averin, *Phys. Rev. Lett.* 88, 207901 (2002).
- <sup>32</sup> A. N. Korotkov, *Phys. Rev. B* 63, 085312 (2001).
- <sup>33</sup> C. W. Gardiner and P. Zoller, *Quantum Noise* (Springer, 2000), 2nd ed.
- <sup>34</sup> M. Field, C. G. Smith, M. Pepper, D. A. Ritchie, J. E. F. Frost, G. A. C. Jones, and D. G. Hasko, *Phys. Rev. Lett.* 70, 1311 (1993).
- <sup>35</sup> D. Sprinzak, Y. Ji, M. Heiblum, D. Mahalu, and H. Shtrikman, *Phys. Rev. Lett.* 88, 176805 (2002).
- <sup>36</sup> J. M. Elzerman, R. Hanson, J. S. Greidanus, L. H. W. van Beveren, S. D. Franceschi, S. T. L. M. K. Vandersypen, and L. P. Kouwenhoven, *cond-mat/0212489* (2002).
- <sup>37</sup> L. S. Levitov, H. W. Lee, and G. B. Lesovik, *J. Math. Phys.* 37, 4845 (1996).
- <sup>38</sup> H. Schoeller and G. Schon, *Phys. Rev. B* 50, 18436 (1994).
- <sup>39</sup> D. Mozysky and I. Martin, *Phys. Rev. Lett.* 89, 018301 (2002).
- <sup>40</sup> R. Ruskov and A. Korotkov, *cond-mat/0202303* (2002).
- <sup>41</sup> U. Gavish, Y. Levinson, and Y. Imry, *Phys. Rev. B* 62, R10637 (2000).
- <sup>42</sup> G. B. Lesovik and R. Loosen, *JETP Lett.* 65, 295 (1997).
- <sup>43</sup> U. Gavish, Y. Imry, Y. Levinson, and B. Yurke, *cond-mat/0211646* (2002).
- <sup>44</sup> R. A. Harris and L. Stodolsky, *Phys. Lett. B* 116, 464 (1982).
- <sup>45</sup> L. N. Bulaeviskii, M. Hruska, and G. Ortiz, *cond-mat/0212049* (2002).
- <sup>46</sup> L. Keldysh, *Sov. Phys. JETP* 20, 1018 (1965).
- <sup>47</sup> A. M. Tsvelik, *Phys. Rev. Lett.* 69, 2142 (1992).
- <sup>48</sup> J. Rammer and H. Smith, *Rev. Mod. Phys.* 58, 323 (1986).
- <sup>49</sup> O. Parcollet and C. Hooley, *cond-mat/0202425* (2002).
- <sup>50</sup> W. Mao, P. Coleman, C. Hooley, and D. Langreth, *cond-mat/0305001* (2003).
- <sup>51</sup> A. Shnirman and Y. Makhlin, *cond-mat/0305064* (2003).
- <sup>52</sup> D. V. Averin, in *Exploring the Quantum (Classical Frontier)*, edited by J. R. Friedman and S. Han (Nova Science Publishers, Commack, NY; *cond-mat/0004364*, 2002).